AiCARR Journal / Vol 63, n. 4, 50 - 55, 2020

Alberto Cavallini[1], Filippo Busato[2]*, Fabrizio Pregliasco[3]

Remarks on the air recirculation in HVAC systems during the SARS-CoV-2 outbreak: the case of all-air ducted plants

Approfondimenti sugli impianti a tutt'aria con ricircolo durante la pandemia SARS-CoV-2

[1] University of Padova; Manens-TiFS SpA, Padova, Italy
[2] Dipartimento di Economia, Telematic University Mercatorum, Rome, Italy
[3] Scienze biomediche per la salute, University of Milan, Milan, Italy

*Corresponding author:
Filippo Busato
Dipartimento di Economia
Telematic University Mercatorum
Piazza Mattei 10
00186 Roma, Italy
filippo.busato@unimercatorum.it
tel +39 347 1207174

DOI: 10.36164/AiCARRJ.63.04.03

Abstract

The SARS-CoV-2 pandemic has aroused great interest in the HVAC community, both as regards to the design of new systems and for the management and operation strategies of the existing ones. The risk management plays a key role in all-air systems based on air recirculation among segregated spaces. Following an analytical approach, this paper assesses the infection risk in several HVAC systems layouts. It takes into account the role of air renewal and recirculation and the gain made possible by means of virus charge removal or deactivation (through filtration or other technologies such as UV-C irradiation, ionisation …), with special regard to the management of airflows that depends on the chosen plant layout.

Keywords:
- All-air ducted plants
- Air recirculation
- SARS-CoV-2 Pandemic

Sommario

La pandemia di SARS-CoV-2 ha destato grande interesse nel mondo della climatizzazione per quanto riguarda la progettazione dei nuovi impianti e la gestione degli impianti esistenti. I temi che sono stati posti in evidenza riguardano anche la gestione del rischio negli impianti a tutt'aria che prevedono il ricircolo dell'aria tra ambienti diversi. Questo articolo valuta, secondo un approccio analitico, le probabilità di contagio per diverse configurazioni impiantistiche, considerando il ruolo del ricircolo dell'aria e le possibilità di miglioramento date dalla rimozione o disattivazione (per filtrazione o altre tecnologie come irradiazione UV-C, ionizzazione …) delle cariche virali, ponendo particolare attenzione alle modalità di gestione delle portate d'aria in relazione agli schemi impiantistici adottati.

Parole chiave:
- Impianti a tutt'aria
- Ricircolo
- Pandemia SARS-CoV-2

NOMENCLATURE

- C: volume concentration of infectious quanta [quanta m^{-3}]
- I: number of asymptomatic infected individuals
- k: removal contribution factor in space by deposition (gravitational settling) [h^{-1}]
- N: total removal factor in the space, $N = \lambda + k + rn$ [h^{-1}]
- NS: total number of people involved (asymptomatic infected individuals + susceptible individuals)
- n_0: initial level of infectious quanta present in volume V (at $t = 0$) [quanta]
- P: probability of infection referred to any exposed susceptible individual
- p: pulmonary inhalation rate by one susceptible individual [m^{3}h^{-1}]
- Q: air flow rate [m^{3}h^{-1}]
- q: infectious quanta emission rate by one asymptomatic infected individual [quanta h^{-1}]
- R^*: average number of susceptible potentially infected people from one contagious person (reproduction index under the specific situation)
- rn: fresh (outdoor) air renewal factor [h^{-1}]
- rc: air recirculation factor [h^{-1}]
- T, t: time [h]
- V: volume [m^3]
- λ: removal contribution factor in space by viral inactivation [h^{-1}]
- η_f: removal/inactivation efficiency in recirculation.

Introduction

The outbreak of SARS-CoV-2 pandemic during the winter season 2019-20 drew immediate and special attention to HVAC systems and their possible contribution to the spread of the disease. According to recent literature, there is a large chance that the virus can survive as airborne [1]. A review study [2] highlights how different factors such as ventilation rates, direction of airflows, and relative position of susceptible and infected individuals can affect the probability of infection in the indoor environment.

To assess the risk of a pandemic, one must refer to an infection model for aerosol carried particles. According to the current knowledge about the virus, the preferable model suitable to be adopted [3] is the Wells-Riley model, as widely supported by recent literature [4].

The present work, by means of mass and concentration balance of airflows in all-air HVAC systems, calculates the pathogen concentration, the outcoming infection probability and the number of potentially infected individuals for different space layouts of segregated rooms, each one served by the same all-air HVAC system.

The main purpose of this paper is to help building a conscious risk assessment plan in HVAC systems for designers, manufacturers, building owners and building managers.

Method and input data

According to the Wells-Riley model [4], the probability for a susceptible individual to contract a disease via aerosol infection follows a Poisson probability function according to Equation 1:

$$P = 1 - e^{-p \cdot \int_0^T C_I(t)dt}$$

Equation 1 – Wells-Riley probability model

Equazione 1 – Modello probabilistico di Wells-Riley

where the absolute value of the exponent of e is the dose of quanta received by a susceptible individual during the exposure time T. In fact in equation 1 p is the pulmonary airflow [m^3/h], $C_I(t)$ the instantaneous (at time t) concentration of infectious doses [quanta/m^3] in the environment (considered as well-mixed), and T [h] is the total time of exposure. The outcoming probability P is a real number in the interval [0; 1].

By implementing the Gammaitoni-Nucci model [5] to this layout, one can evaluate C_I as follows:

$$C_I = \frac{q \cdot I}{N \cdot V} + \left(\frac{n_0}{V} - \frac{q \cdot I}{N \cdot V} \right) \cdot e^{-N \cdot t}$$

Equation 2 – Gammaitoni-Nucci formula

Equazione 2 – Formula di Gammaitoni-Nucci

Equations 1 and 2 with $n_0 = 0$ yield for the probability of infection P:

$$P = 1 - exp\left[\frac{q \cdot I \cdot p}{V} \left(\frac{1 - N \cdot T - e^{-N \cdot T}}{N^2} \right) \right]$$

Equation 3 – Probability of infection for a susceptible individual

Equazione 3 – Probabilità di infezione per una persona suscettibile

Here below, this paper will apply this model (with all connected assumptions, in particular well-mixed environments) in simulating some HVAC layouts of office buildings. Consequently, the level of activity of all involved individuals is taken in the category <light activity – speaking>.

Among all the input parameters required for the application of the above model, the infectious quanta emission of an asymptomatic infected individual related to the SARS-CoV-2 virus is certainly the most uncertain and controversial one, with a huge variation range.

At present, the only data available of q specifically related to SARS-CoV-2 virus come from a single source, Buonanno *et al.* [4, 6, 7]. Still in [4] these authors propose a forward emission approach in order to estimate the quanta emission rate of an infected individual based on the viral load in the sputum and the concentration of droplets expired during different activities. In this same paper, these authors analyze the worst-case scenario in the presence of an asymptomatic SARS-CoV-2 individual in some microenvironments: a pharmacy, a supermarket, a restaurant, a post office and a bank. In all cases, the value assumed for the quanta emission rate was q = 142 quanta h^{-1} (147 quanta h^{-1} in [6]), associated with a pulmonary rate p = 0.96 m^{3}h^{-1} (0.54 m^{3}h^{-1} in [6]).

In a subsequent preprint (Buonanno *et al.* [7]), the same authors present a novel approach for quantitative assessment of the infection risk, based on the determination, through Monte Carlo simulations, of the probability density functions of quanta emission rate, of quanta concentration and of infectious dose inhaled by a susceptible individual. For a simplified estimate, such as the one used in this work, they suggest adopting, for the asymptomatic infected individual's quanta emission rate, the 85th percentile of the quanta emission rate of their probability density function. For the activity <light exercise-speaking>, according to [8] the coherent value is q = 26.3 quanta h^{-1} (to highlight the strong dependence of this parameter on the activity level, the value suggested for <light exercise-loudly speaking>, is q = 170 quanta h^{-1}, while for <light exercise-oral breathing>, q = 5.6 quanta h^{-1}).

In the same preprint, Buonanno *et al.* [7] make a retrospective assessment of two documented Covid-19 outbreaks: in a restaurant in Guangzhou (China) and at a choir rehearsal in Skagit Valley

AiCARR Journal / Vol 63, n. 4, 50 - 55, 2020

(Washington State, USA). In the first case, the backward calculation of the contagious individual's quanta emission rate yields $q = 61$ quanta h^{-1}; this value, for an emitting individual speaking during light exercise, is very close to the 94th percentile value of the probability density function of q (62.2 quanta h^{-1}). In the case of the choir rehearsal, the backward calculation yields $q = 341$ quanta h^{-1}, value close to the 93rd percentile of the probability density function of q of an infected individual while singing (353 quanta h^{-1}). These examples show that, referring to the 85th percentile value of the probability density function of q of the Buonanno *et al.* Monte Carlo analysis is a basic choice far from reproducing a worst-case scenario.

However, the value of the quanta emission rate used in the simulations presented in this work comply with the suggestion given by Buonanno *et al.* [7], that is $q = 26.3$ quanta h^{-1}.

As to the pulmonary inhalation rate p, Adams (as reported in Buonanno et al. [5]) gives the following values, averaged between males and females: 0.49 m^{3}h^{-1} (resting), 0.54 m^{3}h^{-1} (standing), 1.38 m^{3}h^{-1} (light exercise), 2.35 m^{3}h^{-1} (moderate exercise) and 3.30 m^{3}h^{-1} (heavy exercise). All the simulations reported in this work adopt the conservative value $p = 0.8$ m^{3}h^{-1}.

Regarding the removal contribution factors λ (due to space viral inactivation) and k (due to gravitational settling), again the values assumed in the simulations illustrated below comply with the indications in Buonanno *et al.* [5]: $\lambda = 0.63$ h^{-1} (based on SARS-CoV-2 half-life of 1.1 h) and $k = 0.24$ h^{-1} (based on a height of the emission source of 1.5 m).

Finally, the values assumed for the air recirculation factor rc and the outdoor fresh air renewal factor rn comply with the current design practice; extreme values are able to evidence the trend of the simulation results.

Due to the high uncertainty of some of the input data (for the quanta emission rate q, probably even at factor of 5), the readers are advised to look at the simulation numerical results with caution. At this stage of knowledge of this particular disease, it is far more important to look at the trend and variations of the simulation results, consequence of variation of the input parameters or as the effect of control measures.

All-air multi-room AC plants with air recirculation

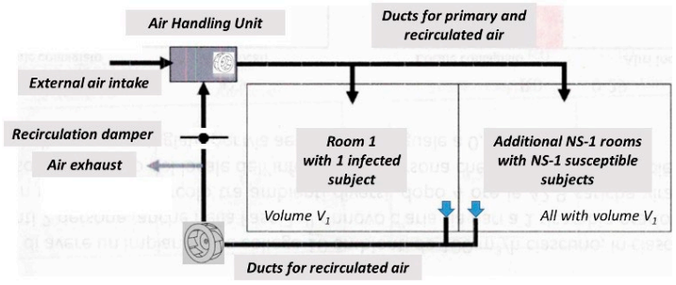

Source: AiCARR

Figure 1 – Sketch of a multi-room HVAC plant with air recirculation

Figura 1 – Schema di impianto a tutt'aria con ricircolo tra ambienti

The sketch in Figure 1 represents an office building multi-room AC all-air plant with air recirculation among the *NS* separated rooms, each one of volume $V_1 = 50$ m^3 and each one with a single occupant. Room 1 accommodates an asymptomatic contagious individual, while in the remaining *NS-1* rooms *NS-1* susceptible individuals are equally distributed. All individuals stay in their office for $T = 8$ hours. For the moment the simulation refers to the assumption that air recirculation brings about no additional removal or inactivation of the infectious quanta.

To model the spreading of the disease in this situation, one can resort to two different models, here dubbed the *uniform model* and the *segregated model*, as illustrated below.

The uniform model

It can be assumed that the effect of the air recirculation among all rooms is equivalent to eliminating the partitions separating the different spaces: all rooms can be treated together as a single well-mixed space of total volume $V = NS \cdot V_1$, and so equations 2 and 3 can be directly applied to this total volume. Figures 2, 3 and 4 illustrate the results of this procedure as a function of the number of different rooms (or the number of people) *NS* involved.

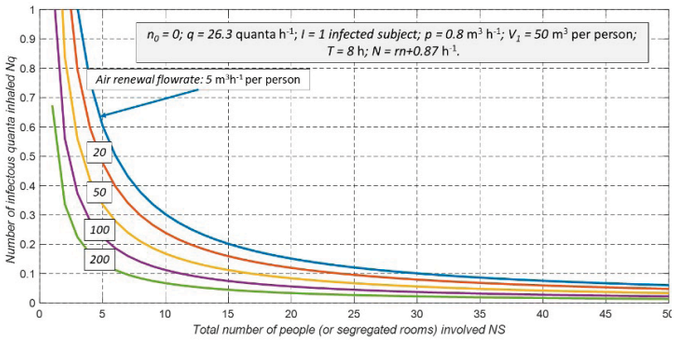

Figure 2 – Concentration of infectious doses inhaled after 8 h

Figura 2 – Concentrazione delle cariche virali dopo 8 h

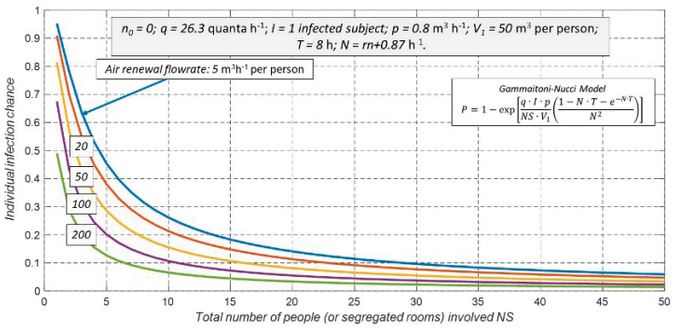

Figure 3 – Probability of infection for each asymptomatic individual after 8 h

Figura 3 – Probabilità di infezione per un asintomatico dopo 8 h

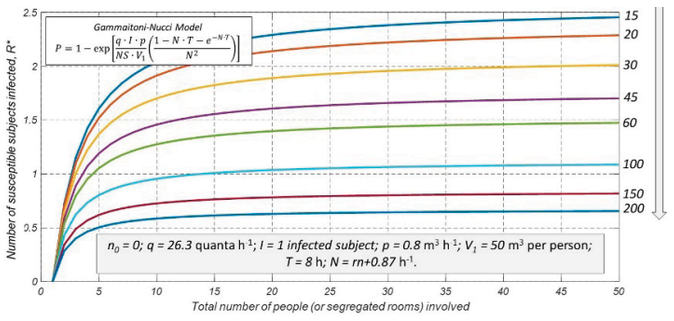

Figure 4 – Number of susceptible individuals infected after 8 h

Figura 4 – Numero di persone suscettibili infettate dopo 8 h

Figure 2 gives the number of infectious quanta inhaled by any susceptible individual during the 8-hour working period, showing the dependence of this quantity on the fresh air renewal airflow, while Figure 3 reports the corresponding infection probability *P* for any exposed susceptible individual. Finally Figure 4 shows the reproduction index $R^* = P \cdot (NS-1)$, that is the total number of people potentially infected. It can be appreciated that this index always increases with the number of individuals involved, although the probability of infection for any susceptible individual decreases when the total number of people involved increases.

The segregated model

The uniform model illustrated above faces some strong limitations and it is over-penalising: it considers the environment as it was a single room, with no difference in infectious quanta concentration between the room with the infected individual and the other spaces. This condition calls for an infinite internal air recirculation; this is the only way to guarantee the "well-mix" conditions among all the rooms. It clearly represents a limit case, when the air recirculation factor is much higher than the air renewal factor, $rc >> rn$.

A big step forward in the modelling consists in retaining physically segregated spaces; the only connection among different rooms is given by the all-air ducted HVAC plant, providing airflows with *rn* [h^{-1}] as the renewal factor and *rc* [h^{-1}] as the recirculation factor in each room. Figure 5 shows the sketch of this model.

Equation 4 refers to the concentration balance in the infected room C_I, while Equation 5 gives that of the other rooms, where C_S is the concentration of viral quanta in the susceptible people's rooms, and C_R is the quanta concentration of the recirculated air. All spaces are considered as perfectly mixed.

$$\frac{\partial C_I}{\partial t} = \frac{q \cdot I}{V_1} + rc \cdot C_R - (rc + N) \cdot C_I$$

Equation 4 – Concentration balance for the room of the infected individual

Equazione 4 – Bilancio di concentrazione per il locale dell'individuo infetto

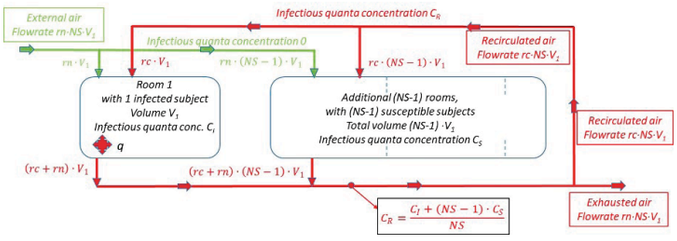

Figure 5 – Concentration and flow balance model

Figura 5 – Modello di bilancio di concentrazione e portata

$$\frac{\partial C_S}{\partial t} = rc \cdot C_R - (rc + N) \cdot C_S$$

Equation 5 – Concentration balance for the *NS-1* susceptible individuals' rooms

Equazione 5 – Bilancio di concentrazione per gli NS-1 *locali degli individui suscettibili*

$$C_R = \frac{C_I + (NS - 1) \cdot C_S}{NS}$$

Equation 6 – Concentration balance of recirculated air

Equazione 6 – Bilancio di concentrazione per l'aria ricircolata

By including the recirculation Equation 6 in the model, the result is a first order PDAE system reducible to a PDE system and symbolically solvable, whose explicit solution is hereby omitted for the sake of brevity. The system can be numerically solved by Matlab.

Figure 6 shows the results of the application of the segregated model in terms of the reproduction index R^* vs. the total number of people involved *NS*.

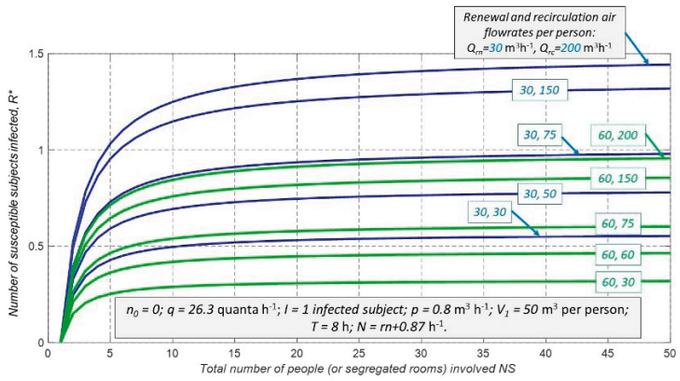

Figure 6 – Number of susceptible individuals infected after 8 h

Figura 6 – Numero di persone suscettibili potenzialmente infettate dopo 8 h

The dependence of R^* on both the fresh air renewal rate and the air recirculation rate can be appreciated.

The effect of virus removal/inactivation in the supply duct

It is also possible to extend the segregated-room model in order to account for the presence of filtration or inactivation devices (high efficiency filters, UV-C irradiation, photocatalytic oxidation, plasmacluster or negative air ionisation) in the air supply duct (after the mixing plenum). If one assumes a removal/deactivation efficiency η_f in the interval [0; 1], than a multiplication factor of (1- η_f) must be introduced in the C_R formula in Equation 6. Figures 7 to 10 show the relative results, referred to the case of double-occupancy rooms, to also show the effect of virus removal/deactivation on the infector's susceptible roommate. As it can be found in the plot labels from Figure 7 to Figure 10, the case refers to 2 people in room 1 (1 infected and 1 susceptible person) of volume $2V_1$, while other *NS-2* people are segregated in the other rooms; again each individual has at his disposal a volume $V_1 = 50$ m^3. Therefore the number of potentially infected individuals accounts for 1 susceptible in room 1 and *NS-2* susceptible individuals in the remaining rooms; this number can't reach the value of 0 even for $rc = 0$, because of the presence of the infector's roommate.

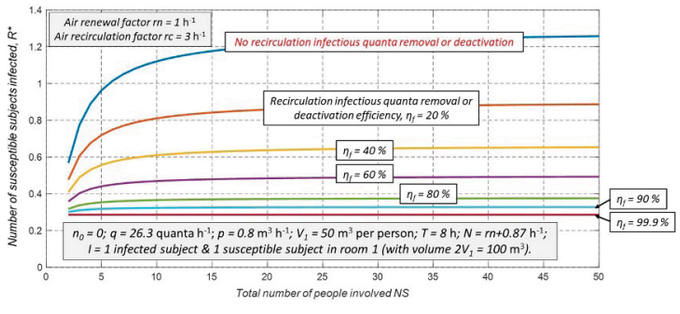

Figure 7 – Effect of different removal/inactivation efficiencies

Figura 7 – Effetto delle diverse efficienze di rimozione/inattivazione

AiCARR Journal / Vol 63, n. 4, 50 - 55, 2020

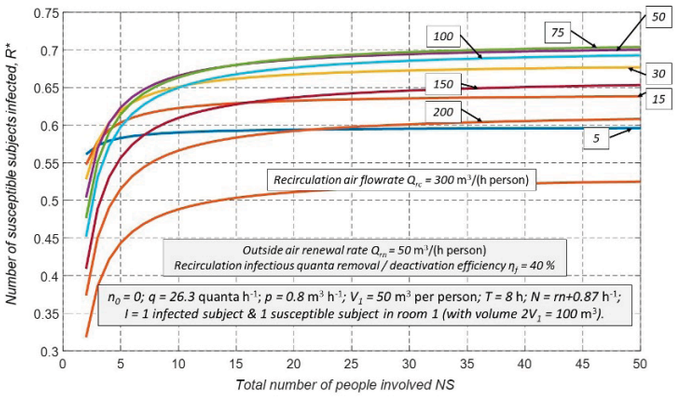

Figure 8 – **Effect of different recirculation rates with a removal/inactivation efficiency of 40%**

Figura 8 – Effetto del tasso di ricircolo per una efficienza di rimozione/inattivazione del 40%

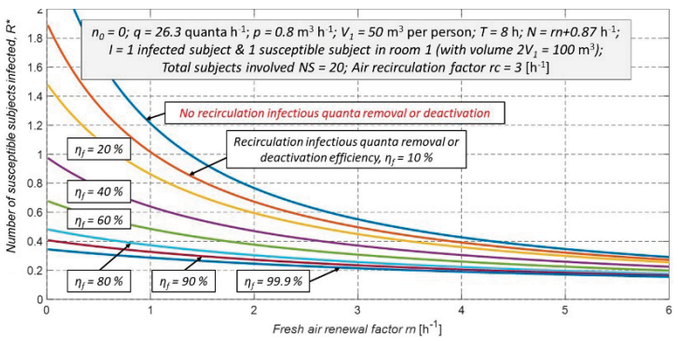

Figure 9 – **Effect of the outdoor air renewal factor for different removal/inactivation efficiencies**

Figura 9 – Effetto del tasso di rinnovo d'aria per diverse efficienze di rimozione/inattivazione

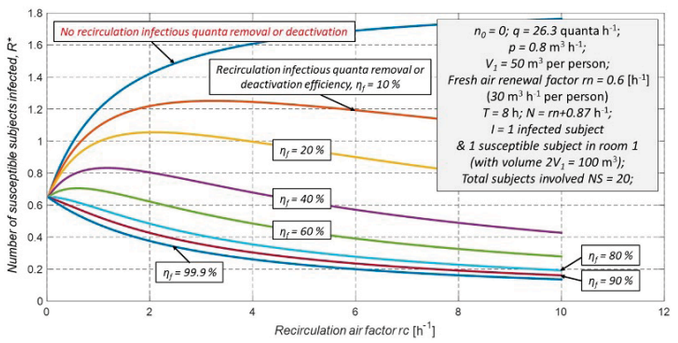

Figure 10 – **Effect of the air recirculation factor for different removal/inactivation efficiencies**

Figura 10 – Effetto del tasso di ricircolo per diverse efficienze di rimozione/inattivazione

It is interesting to observe that, in the case illustrated in Figure 8, the reproduction index *R** reaches a maximum when the air recirculation rate increases, then decreasing at higher recirculation rates. This fact, also evident in Figure 10 for removal/deactivation efficiencies less than 80%, is due to the double contrasting effect of increasing air recirculation when air purification devices are present. On one side, air recirculation spreads the virus to the rooms occupied by the susceptible individuals; on the other side, air recirculation helps removing/inactivating the virus content in all the rooms.

The effect of common spaces ventilation management

By suitable adaptation of equations 3 to 5, it is possible to extend the model to specific real application cases, considering as well common spaces and a likely scheduling for room occupation. Figure 11 sketches the situation where, in addition to *NS* single-occupancy offices, there are common spaces (corridor, service rooms), with a volume amounting to 20% of the total volume of the offices served by the primary air HVAC plant. The infected individual is in room 1, and, along with his workmates, spends a fraction of the working time (8 hours per day) in the common areas. All the occupants leave the building for one-hour lunch break after 4 h in the morning, and come back 4 h in the afternoon. An exhaust fan in the service rooms extracts a fraction of the whole air, while the air-handling unit supplies the full 100% fresh air to the single offices only; there is no direct supply air to the corridor nor to the service rooms.

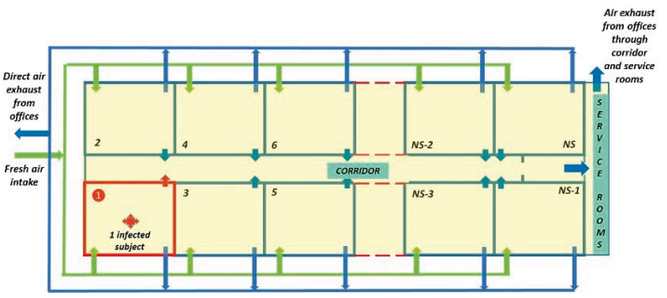

Figure 11 – **Physical model including common spaces**

Figura 11 – Modello fisico che include aree comuni

Figure 12 shows a timeline of the viral quanta concentration in the room of the infected individual, while Figure 13 shows the timeline of quanta concentration in the well-mixed common spaces (corridor, service rooms). Therefore the assumption is made that the infected person, as well as the other workers, spends 20 min during the working time in the common spaces; the plots refer to a total number of people involved *NS* = 10, an air renewal factor *rn* = 1 h⁻¹, and 10% ventilation air exhausted from the common rooms.

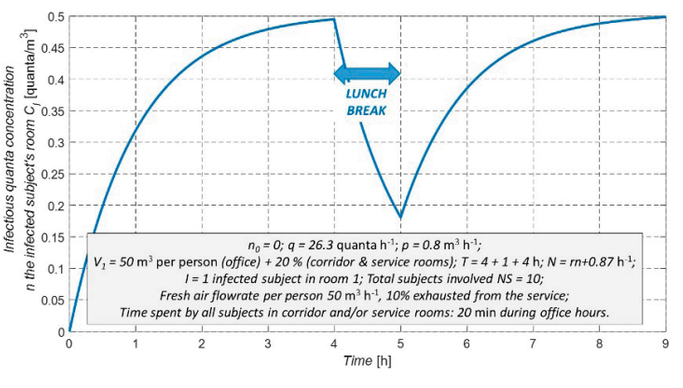

Figure 12 – **Concentration of viral quanta in the infected room 1**

Figura 12 – Concentrazione delle cariche virali nel locale dell'infetto

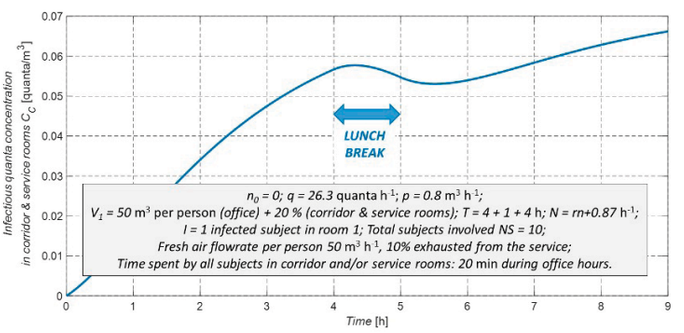

Figure 13 – **Concentration of viral quanta in the corridor and service rooms**

Figura 13 – Concentrazione delle cariche virali nelle aree comuni

The following plot in Figure 14 shows how the presence of the infected individual in the common spaces and the fraction of ventilation air exhausted from the service rooms affect the number of susceptible people that are expected to be infected after the day. It is then interesting to see in Figure 15, how the fraction of air extracted from the common spaces can actively reduce the number of infected individuals.

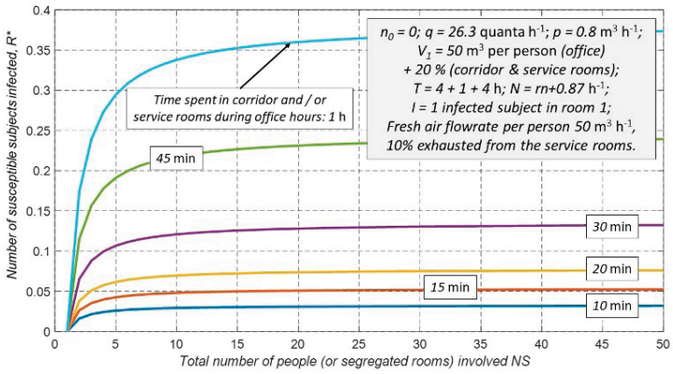

Figure 14 – Susceptible individuals infected as a function of the time all persons spend in the common spaces

Figura 14 – Numero di persone potenzialmente infettate in funzione del tempo trascorso nelle aree comuni

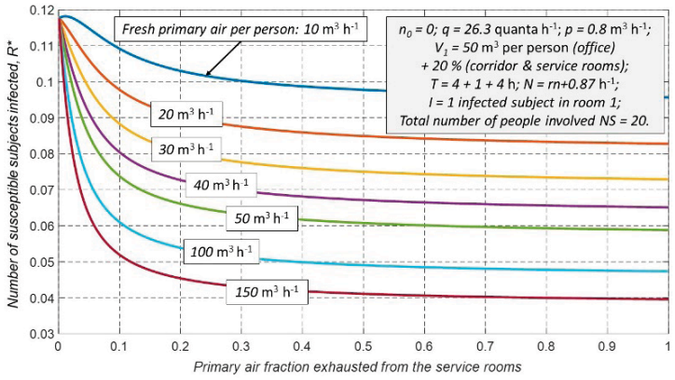

Figure 15 – Susceptible individuals infected as a function of air renewal and of the fraction of air extracted from the common spaces

Figura 15 – Numero di persone potenzialmente infettate in funzione del tasso di rinnovo e della frazione di portata estratta dalle aree comuni

Conclusions

The aim of this work was to calculate, by means of concentration balances and the Wells-Riley infection model, the infection probability in all-air ducted HVAC systems with air recirculation. After a brief analysis of a simple model (already considered in the specific literature), several improvements to the model were added. As shown, the results highlight an important outcome related to HVAC plants with air recirculation: the sole effect of dilution in multiple rooms is not enough to compensate for the increased number of involved susceptible individuals. On the other hand, high air renewal rates can strongly reduce the risk of infection at a given recirculation rate; furthermore filtration (or other equivalent technologies to inactivate the virus from recirculated airflows, such as UV-C irradiation or ionisation) is a very powerful tool to reduce the infection probability, especially if coupled to high recirculation rates. Finally, it is very important to consider, in real case applications, the management of airflows in both segregated and common spaces, which can heavily modify the behaviour of the system.

CONFLICT OF INTEREST

The Authors declare the absence of economic or other types of conflicts of interest in all of the phases of the paper preparation.

REFERENCES

[1] Morawska L., Cao J., Airborne transmission of SARS-CoV-2: The world should face the reality. Environment International 2020; 139; 105730; https://doi.org/10.1016/j.envint.2020.105730

[2] Ai Z.T., Melikov A. K., Airborne spread of expiratory droplet nuclei between the occupants of indoor environments: a review. Indoor air 2018, https://doi.org/10.1111/ina.12465

[3] Sze To G.N., Chao C.Y.H., Review and comparison between the Wells–Riley and dose-response approaches to risk assessment of infectious respiratory diseases. Indoor air 2010; 20; 2-16; https://doi.org/10.1111/j.1600-0668.2009.00621.x

[4] Buonanno G., Stabile L., Morawska L., Estimation of airborne viral emission: Quanta emission rate of SARS-CoV-2 for infection risk assessment. Environment International 2020; 141; https://doi.org/10.1016/j.envint.2020.105794

[5] Gammaitoni L, Nucci M. C., Using a Mathematical Model to Evaluate the Efficacy of TB Control Measures. Emerging Infectious Diseases 1997, vol. 3, n. 3, 335-342.

[6] Buonanno G., Stabile L., Morawska L., Estimation of airborne viral emission: Quanta emission rate of SARS-CoV-2 for infection risk assessment. https://doi.org/10.1101/2929.04.1220062828

[7] Buonanno G., Stabile L., Morawska L., Quantitative assessment of the risk of airborne transmission of SARS CoV-2 infection: prospective and retrospective applications. medRxiv preprint doi: https://doi.org/10.1101/2020.06.0120118984. After the submission of this manuscript to the AJ Editor, the peer-reviewed article from the above manuscript has been published:
Buonanno G., Stabile L., Morawska L., Quantitative assessment of the risk of airborne transmission of SARS CoV-2 infection: Prospective and retrospective applications. Environment International 145 (2020); https://doi.org/10.1016/j.envint.2020.106112

[8] Jimenez J. L., COVID-19 Aerosol Transmission Estimator; https://cires.colorado.edu/news/covid-19-airborn-transmission-tool-available